Hindawi
Journal of Sensors
Volume 2019, Article ID 8014102, 10 pages
https://doi.org/10.1155/2019/8014102

Research Article

Cross-Sectional Loss Quantification for Main Cable NDE Based on the B-H Loop Measurement Using a Total Flux Sensor

Ju-Won Kim,[1] **Junkyeong Kim**,[2] **and Seunghee Park**[1]

[1]*School of Civil, Architectural Engineering and Landscape Architecture, Sungkyunkwan University, Suwon, Gyeonggi-do 16419, Republic of Korea*
[2]*Research Strategy Team, Advanced Institute of Convergence Technology, Gyeonggi-do 16229, Republic of Korea*

Correspondence should be addressed to Seunghee Park; shparkpc@skku.edu

Received 4 April 2019; Revised 2 July 2019; Accepted 26 July 2019; Published 9 October 2019

Guest Editor: Lalita Udpa

In the real world, the main cables of suspension bridges are commonly inspected by conducting a periodic visual inspection of the exterior cover of the cable. Although there is a need to conduct a nondestructive evaluation (NDE) of the damage of the main cable, a suitable NDE technique has not yet been developed due to the large diameter and low accessibility of the cable. This study investigates a magnetic sensing cross-sectional loss quantification method that can detect internal and external damage to the main cables. This main cable NDE method applies an extremely low-frequency alternating current (ELF-AC) magnetization method and search coil sensor-based total flux measurement. A total flux sensor head consists of a magnetization yoke and a search coil sensor. To magnetize the main cable, a magnetic field was generated by applying a triangular ELF-AC voltage to the electromagnet yoke. The sensing part measures the magnetic flux that passes through the search coil, and the B-H loop was then obtained using the relationship between the ELF-AC voltage that has been input and the total flux that was measured. Also, the cross-sectional loss can be quantified using a variation of magnetic features from the B-H loop. To verify the feasibility of using the proposed NDE technique, a series of experiments were performed using a main cable specimen with a gradual increase in the cross-sectional loss. Finally, the relationship between the cross-sectional loss and extracted magnetic feature was determined and used to quantify the cross-sectional loss via the proposed method.

1. Introduction

In suspension bridges, steel cables are the core supporting materials that suspend most of the load of the structure. However, cross-sectional damage can occur in steel cables due to external causes, including corrosion and fracture. And it can lead to stress concentration as a direct cause of structural failure due the rapid expansion of the damage. Therefore, a suitable nondestructive evaluation (NDE) method is needed to inspect the initial stages of damage in a steel cable so that accidents can be prevented. However, it is difficult to diagnose cables since the damage in cable can be invisible and inaccessible.

To overcome these limitations, this research proposes a noncontact NDE technique incorporating magnetic sensing technology to exploit the ferromagnetic characteristics of steel cables. Magnetic sensors have been extensively used to monitor the safety of structures due to their great reproducibility and reliability [1–3]. Various types of magnetic sensors exist to measure various magnetic properties, and the appropriate magnetic properties obtained from the measured magnetic signals can be used to inspect the structure according to the characteristics of the targeted object [4–7]. Although magnetic sensing techniques have not been commonly used to inspect large-scale civil infrastructure, researchers have recently investigated the use of magnetic sensing methods for large infrastructure, including railroads, pipelines, and suspension bridges [3, 8–10].

Typically, the magnetic flux leakage (MFL) method is an optimal technique for use with continuum structures that have a constant shape in their cross-section, such as railroads and pipelines, and it has been utilized to inspect steel wire ropes for elevators and cranes and for other applications [11–16].

However, the hidden damage within large-diameter cables has not been detected since the MFL technique can only detect a local defect near the surface. Therefore, the MFL method is not a suitable NDE method to inspect the main cables of suspension bridges with a very large diameter. In addition, research and development to replace conventional visual inspection methods have not been actively conducted due to the large size of the main cables.

To overcome such limitations, a new method was proposed to inspect the whole cross-section, including the internal and external section. The proposed technique incorporates an extremely low-frequency alternating current (ELF-AC) magnetization method with total flux measurement using a search coil sensor to obtain magnetic hysteresis loops (B-H loop) according to each condition of the main cable [17]. From the obtained B-H loops, magnetic properties were extracted to quantify the cross-section of the cable, and a quantification algorithm using a variation of the extracted magnetic properties is induced to estimate the rate of cross-sectional loss of the main cables. The feasibility of the proposed main cable NDE technique has been verified through a series of experimental studies using a large-diameter cable specimen with inflicted artificial loss of strands.

2. Theoretical Background

2.1. Magnetization Using an Electromagnetic Yoke. When the material is positioned within a strong external magnetic field, ferromagnetic materials can be magnetized because the magnetic domains within the material are aligned [18]. When a stronger magnetic field is applied to the material, more domains are aligned, and this state is said to be magnetically saturated when all magnetic domains are aligned.

When the solenoid coil is used for the magnetization process, the electric current flows through the carrying conductor in coil; a strong concentrated magnetic field is then generated at the center of the solenoid coil. The strength of the magnetic field in the coil increases as the applied current increases with additional turns of the coil [19]. The magnetic field generated inside the solenoid coil is very helpful to magnetize the ferromagnetic materials to inspect the magnetic domain [9].

However, the magnetization method using a solenoid coil makes it difficult to apply for the continuum specimen in the real field due to its closed-loop shape.

Therefore, a yoke-type electromagnet is utilized in this study to replace the solenoid and improve the applicability in the field. Typically, an electromagnet yoke consists of a solid steel bar core and a solenoid that is winded around the core, as shown in Figure 1.

When an electric current flows through a solenoid around the steel bar, a magnetic flux is exhibited at the steel bar core of the magnetization yoke. When the magnetic flux passes through the magnetization yoke, both ends of the yoke become the north pole and the south pole, respectively. As shown in Figure 1, a magnetic field is then induced between the north and south poles of the yoke.

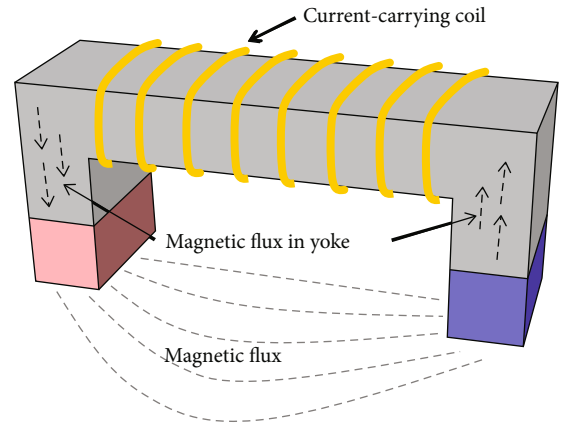

Figure 1: Yoke-type electromagnet for magnetization.

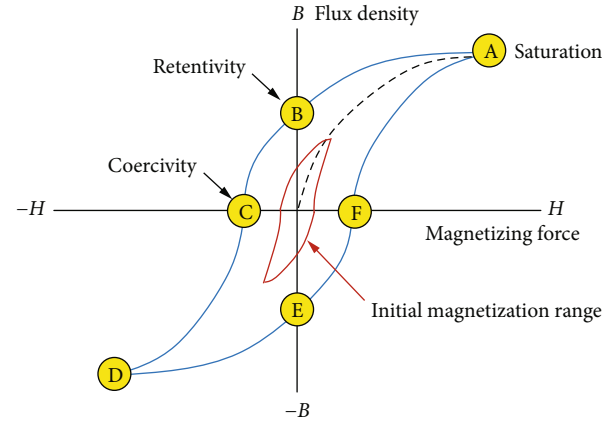

Figure 2: B-H loop (magnetic hysteresis loop) [21].

This magnetic field can be used to indirectly induce a magnetic field in a material so that the specimen can be magnetized for inspection.

In this study, the ELF-AC voltage is applied to magnetize the entire specimen of the main cable using an electromagnetic yoke. The magnetic field produced via ELF-AC can generally penetrate the entire cross-section of the ferromagnetic materials. ELF-AC is very effective when inspecting the entire cross-section of a large specimen because ELF-AC generates an efficient magnetic field that penetrates deeper into the material.

2.2. Search Coil Sensor-Based Total Magnetic Flux Measurement. The principle of the search coil sensing method is based on Faraday's law of induction [4]. A voltage proportional to the rate of variation of the magnetic flux is generated between the leads of the search coil sensor when the magnetic flux through a search coil changes. The magnetic flux through the search coil will vary if the coil moves through a nonuniform field, or if the coil is in a magnetic field that changes with time. The magnetic flux that reflects the condition of the specimen in the magnetic domain is affected by the cross-sectional area of the specimen, material properties, and so on [5].

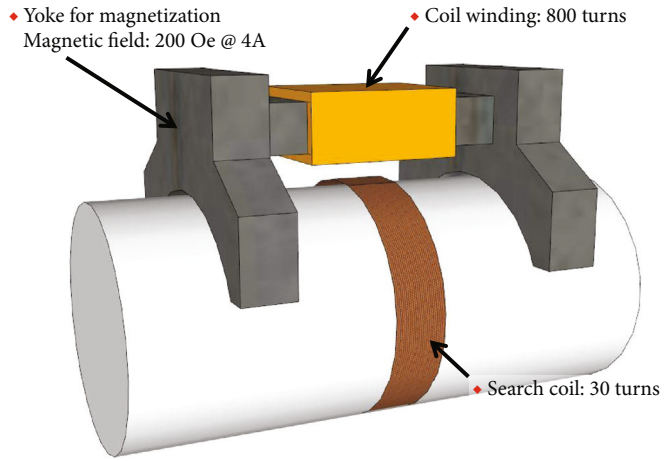

Figure 3: Design of the total flux sensor head.

According to Faraday's law and Lenz's law, the electromotive force generated in a linked search coil by the time variation of the induction is calculated using

$$V_f = -\frac{d\Phi}{dt}, \tag{1}$$

where the total magnetic flux Φ is given as

$$\Phi = NAB, \tag{2}$$

where N is the number of turns of the coil, A is the cross-section of the specimen, and B is the flux density of the specimen.

The magnetic flux density B of the specimen and the induced outer magnetic field H are related as follows:

$$B = \mu_0 \mu_r H, \tag{3}$$

where μ_0 is the related permeability of air and μ_r is the relative permeability of the specimen.

The electromotive force V_f was integrated using the OP amp with the Miller integrator, and the integrated output voltage $V(t)$ is as follows [4, 20]:

$$V(t) = -\frac{1}{RC}\int V_f(t)dt, \tag{4}$$

where RC is the time constant of the integrator. Thus, equation (4) is rewritten as follows:

$$V(t) = \frac{N[\mu_0 \mu_r H]}{RC} A(t). \tag{5}$$

According to equation (5), when the permeability is constant, the output voltage $V(t)$ depends on the cross-section $A(t)$ of the specimen. The output voltage $V(t)$, which is called the total magnetic flux, is measured using a fluxmeter incorporating the OP amp with the Miller integrator.

Table 1: Specification of the total flux measurement system [22].

Search coil diameter	320 mm
Yoke size	$430 \times 440 \times 350$ ($L \times W \times H$) (mm)
Average magnetic path	290 mm
Coil winding	N1: 800 turns, N2: 30 turns
Max current	±14 A
Total flux range	1×10^3 to 2×10^9 Maxwell-turns
Input voltage range	±4 V
Examination time	<60 sec
Magnetizing depth	Entire cross-sectional area
Control program	LabVIEW-based UI

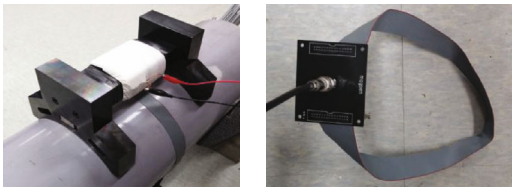

(a) (b)

Figure 4: Fabricated total flux sensor head: (a) magnetization yoke; (b) belt-type search coil sensor.

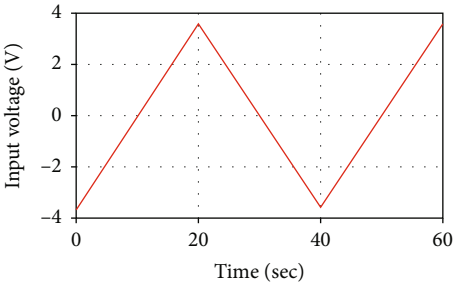

Figure 5: Input voltage shape for magnetization [22].

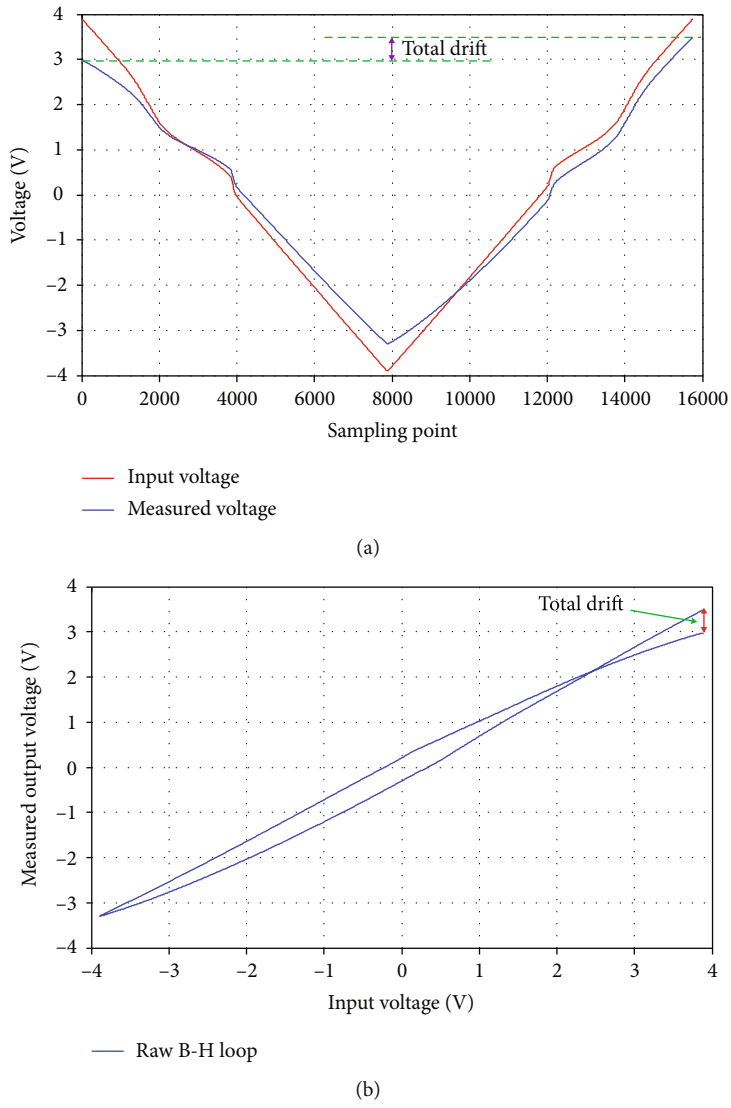

Figure 6: Measured raw signals and raw B-H loop: (a) raw signal; (b) raw B-H loop.

Therefore, the cross-sectional loss can be quantified by measuring the total flux using the search coil sensor and fluxmeter.

2.3. Cross-Sectional Quantification Using a Variation in the Minor B-H Loop. The B-H loop (magnetic hysteresis loop) represents the relationship between the magnetizing force (magnetic field) (H) and induced magnetic flux density (magnetization) (B) [21], as shown in Figure 2.

The B-H loop is obtained by measuring the total flux of a ferromagnetic material while the magnetizing force changes as a cycle. The B-H loop of the whole cycle obtained from a sufficient bipolar magnetic field to make a fully magnetized condition is referred to as a major B-H loop. Utilizing the major B-H loop is the most effective method to conduct the magnetic inspection since the major loop indicates the various magnetic properties of the specimen [21]. However, it is difficult to apply this on site due to the low feasibility since the sensor head required to fully magnetize the real main cable is too big. Therefore, the initial minor B-H loop, the red line in Figure 2, was utilized in this study in place of a major B-H loop to improve the feasibility.

To quantify the cross-sectional loss, the magnetic properties that change according to the cross-sectional loss were extracted. Among the various magnetic properties from the B-H loop, the slope of the B-H loop was extracted and is referred to as the permeability. Permeability is a property of the ferromagnetic material which describes the degree of magnetization of a material in response to a magnetic field. In general, the permeability is used to estimate the tension force of a cable by measuring the voltage from the search coil sensor under the assumption that the constant cross-sectional area is in accordance with equation (5) [4, 20]. Meanwhile, this equation is utilized to estimate the variation in the cross-section $A(t)$ in this study. The cross-section $A(t)$ can be estimated using the measured voltage $V(t)$ when the tension is assumed to be constant.

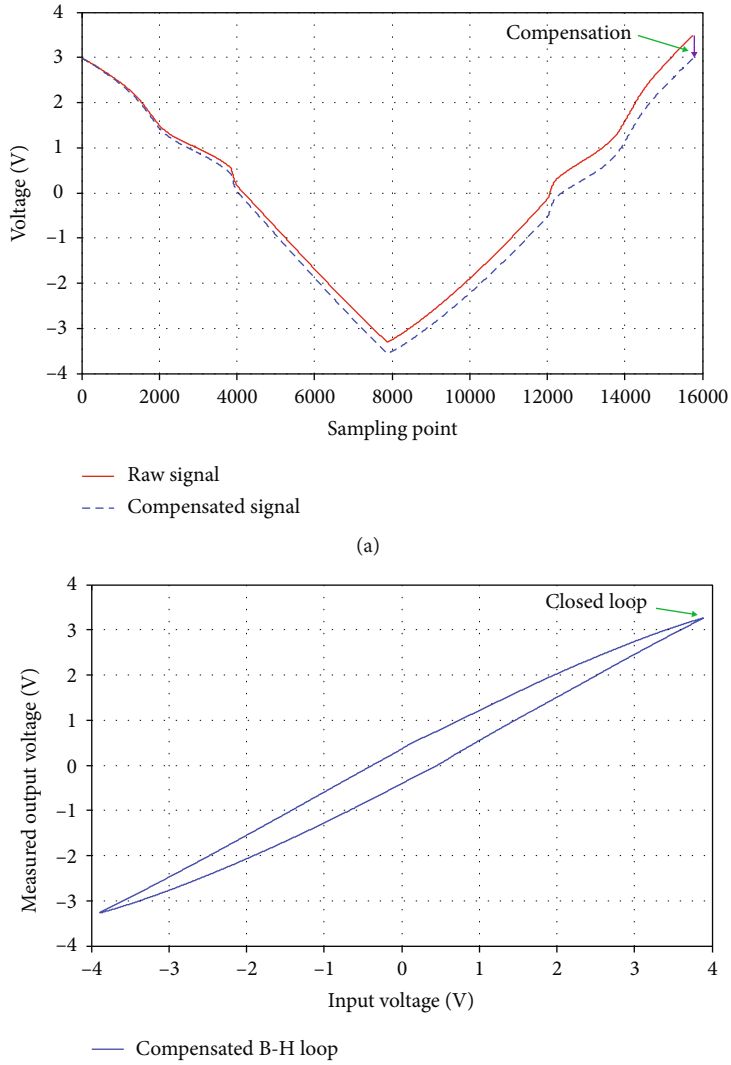

Figure 7: Denoised signal and B-H loop: (a) denoised signals; (b) denoised B-H loop.

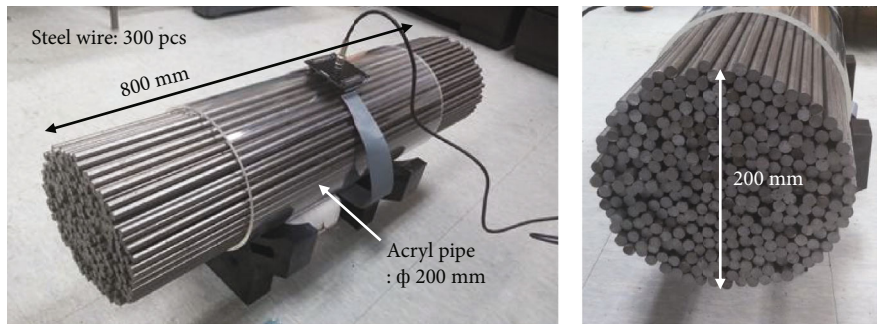

Figure 8: Main cable specimen.

3. System Fabrication for the B-H Loop Measurement

3.1. Fabrication of the Total Flux Sensor Head. Figure 3 shows detailed drawings of the total flux sensor head that was fabricated as described above. It is designed to be suitable for use with a 300 mm diameter main cable. Specific information of the total flux measurement system is described in Table 1.

An electromagnetic yoke consisting of a steel bobbin and a winded solenoid coil is applied to magnetize the large

diameter cable specimen. In addition, the total flux signals were measured using a search coil sensor, and the search coil sensor was configured as an openable belt type using a flexible coil and a PCB board for convenient in situ installation. The fabricated total flux sensor head is displayed in Figure 4.

The magnetization yoke size is 430 mm × 440 mm × 350 mm ($L \times W \times H$), and the coil winding number of the copper coil in the yoke for the magnetization is 800 turns.

The internal diameter of the flexible search coil sensor for sensing the total magnetic flux is 320 mm, and the winding number is 30 turns. The test time for a cycle of the measurement is 60 seconds.

3.2. DAQ Configuration and B-H Loop Acquisition Process. In this system, the ELF-AC voltage is applied to magnetize the entire inside and outside of the specimen. A bipolar power supply generated an ELF-AC voltage, and it is supplied to the primary coil at the electromagnetic yoke to magnetize the main cable specimen.

The cycle of a triangular ELF-AC voltage is supplied to obtain a cycle of the B-H loop in this study. Its amplitude range is ±4 V, and it is supplied to the magnetization yoke for 60 seconds [22]. This voltage can be classified as ELF-AC since it changes very slowly. The wave shape of a triangular ELF-AC voltage applied in the magnetization yoke is shown in Figure 5.

After the magnetizing process, a search coil sensor measures the magnetic flux density from the entire cross-section of the magnetized cable specimen, and the obtained magnetic flux density values are integrated using a fluxmeter to calculate the total magnetic flux.

Since an excessive measurement system is required to obtain a major B-H loop through saturation magnetization of the main cable that has a large size diameter, the voltage range of initial magnetization, shown as the red line in Figure 2, was applied to obtain a minor B-H loop in this study.

Among the characteristics of the B-H loop according to the condition of the cable specimen, the permeability that means the slope of the B-H loop is used to be an index to quantify the variation in the cross-sectional condition.

3.3. Compensation and Denoising Processes to Improve the Quality of the Signals. Figures 6(a) and 6(b) show a sample of the raw signal obtained from the B-H loop. As shown in Figure 6(a), electrical drift occurred during the system operation. This natural drift can disturb the signal and extract the magnetic feature from the B-H loop.

To avoid errors due to drift, a series of denoising processes were performed since the raw signal contains the drift and an offset error. Although this signal processing can induce some distortion in the original B-H loop characteristics, the focus of this study was the index extraction which changes with the cross-section change. Therefore, the following consistent compensation was performed to form the closed B-H loop. This procedure is helpful in providing reference points for index extraction that reflects the B-H loop such as the slope of the B-H loop.

To compensate for the drift error, the total error was divided into a number of sampling points, and the value was added in direct proportion to the sampling point, as shown in Figure 7. In addition, the offset compensation process was performed to facilitate a comparison between the B-H loops from each condition.

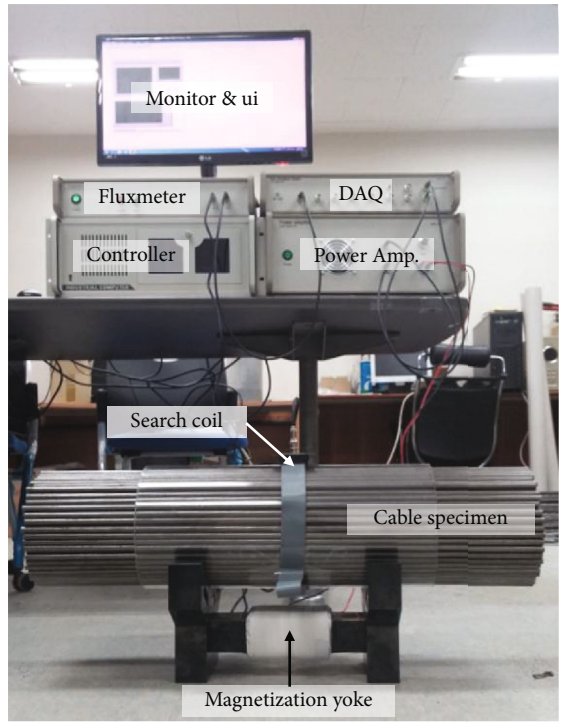

Figure 9: Experimental setup for total flux measurement.

4. Experimental Study

4.1. Experimental Setup and Procedure. A series of experimental studies were performed to examine the capabilities of the cross-sectional loss quantification using the variation of the B-H loop.

A main cable specimen of 200 mm in diameter and 800 mm in length was fabricated for the experimental study, as shown in Figure 8, by filling 300 strands of steel wire in an acrylic pipe-type zig with an internal diameter of 200 mm, as shown in Figure 8. Each strand of the round bar was 10 mm in diameter.

Figure 9 shows the setup for the laboratory experiment. A magnetization yoke and a search coil were installed at the circumferential direction of the specimen. The search coil was fixed to the acrylic case of the specimen when the experiment is carried out since the shape of the search coil can affect the measured signal. A power amplifier to generate the ELF-AC to the wired coil at the magnetization yoke, a fluxmeter to determine the integral of the total flux signal from the search coil sensor, a DAQ, and a controller comprised the measurement system to obtain the B-H loop from the specimen. This measurement system was operated using the LabVIEW user interface.

The test procedure to quantify the cross-sectional loss was the same as that shown in Table 2. To simulate the cross-sectional loss, 30 strands of steel bars were removed

Table 2: Test procedure and steps for the cross-sectional loss.

0% loss	10% loss	20% loss	30% loss	40% loss	50% loss
					

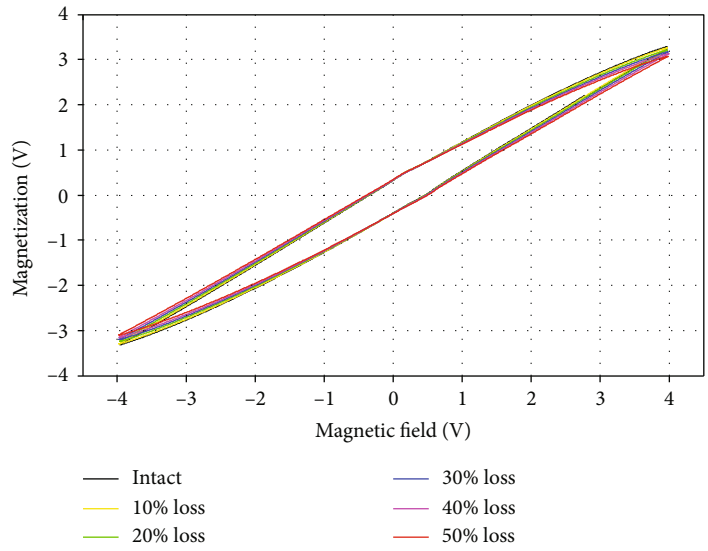

Figure 10: Variation in the B-H loop according to the cross-sectional loss.

at each step from the main cable specimen. Thirty strands of steel bars correspond to 10% of the cross-section of the intact condition, and the experiment was performed in six steps from the intact condition to the 50% loss condition. Using the sensor head and signal measurement system, a cycle of the B-H loop was obtained for a repetition of 10 times in each cross-sectional loss level.

5. Experimental Results

A minor B-H loop from the main cable specimen is obtained at each step of the cross-sectional loss by a cycle of the total flux acquisition and denoised process. The obtained B-H loops using the average value of each case are displayed in Figure 10.

As shown in Figure 10, the dead end of the B-H loops changed gradually. Figure 11 shows the enlarged figure of the dead end of the B-H loops, and it shows that the vertex of the B-H loop decreases progressively, according to the cross-sectional loss level, due to the removal of steel bars.

The variation in the B-H loop implies a variation in various magnetic characteristics according to the specimen's condition, such as permeability, conductivity, and retentivity. Therefore, feature extraction of the magnetic characteristic from the B-H loop is needed to quantify the cross-sectional loss. In this study, the slope of the B-H loop, which means the permeability, was extracted from the B-H loops for each step.

The slope derived from the B-H loop is plotted in Figure 12. The slope of the B-H loop decreases gradually according to the cross-sectional loss, as shown in Figure 12. In addition, the rate of decrease increased slightly, and this was presumed based on the nonconstant magnetization strength due to the biased position of the magnetization yoke.

To improve the accuracy of the damage detection, the cross-sectional loss level between each step was reduced to 1.67%. Figures 13 and 14 show the variation in the B-H loops and the variation curve of the slope of the B-H loop, respectively.

As shown in Figures 13 and 14, the slope decreases with the cross-sectional loss, as with the case of the 10% reduction, and this result shows that a cross-sectional loss of less than 2% can be detected.

In addition, the change in the relation curve in Figure 14 is similar to the change in the range of 0% to 10% of the curve in Figure 12. Therefore, the data sets obtained through the two cases of experiments are seen to have reliability through similarity between the data sets.

These results indicate that the proposed cable inspection method using the total flux sensor can quantitatively diagnose the cross-sectional loss of the large-diameter cable.

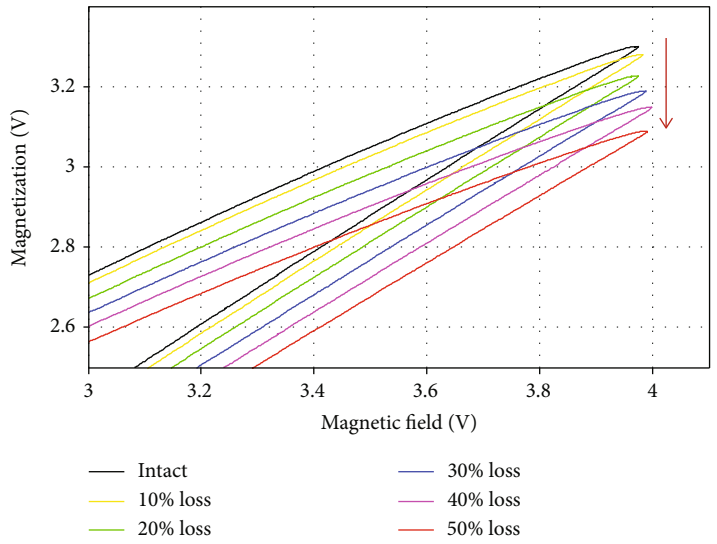

Figure 11: Enlarged plot of the dead end of the B-H loops.

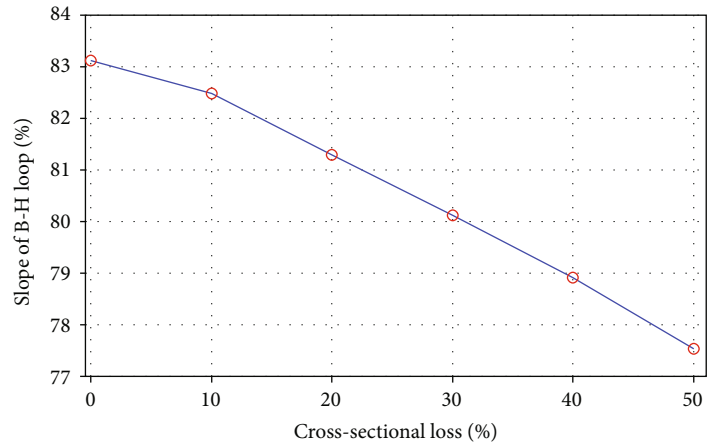

Figure 12: Relation between the extracted feature and the cross-sectional loss.

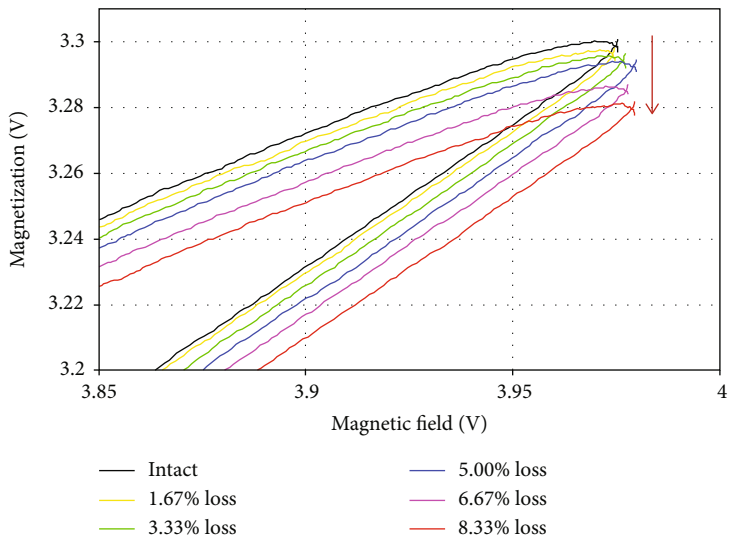

Figure 13: Enlarged plot of the dead end of the B-H loops of the 1.67% reduction case.

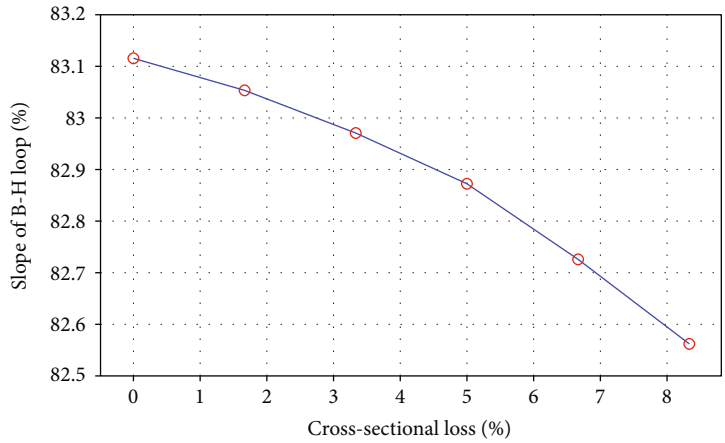

Figure 14: Relation between the extracted feature and cross-sectional loss of the 1.67% reduction case.

6. Conclusions

A main cable NDE method is proposed incorporating ELF-AC magnetization using an electromagnet yoke with a total flux measurement via a search coil to diagnose the cross-sectional loss of the main cable in suspension bridges. A magnetic sensor head for the total flux measurement was fabricated incorporating an electromagnet yoke and a search coil sensor to obtain a B-H loop from the main cable. A series of experimental studies were performed using the fabricated total flux sensor head and the main cable specimen that can remove part of the wire. For each cross-sectional loss level, a B-H loop according to the cross-sectional loss is obtained by using the relationship between the input ELF-AC voltage signal and the measured total flux signal. The slope of the B-H loop, which reflects the permeability, was extracted at each obtained B-H loop to quantify the variation in the B-H loop. This experimental result shows that the slope of the B-H loop decreases gradually according to the stepwise cross-sectional loss and also shows that a constant relationship exists between the variation of the B-H loop and the cross-sectional loss of the main cable specimen. The total flux sensing-based main cable NDE technique can be utilized to diagnose cross-sectional loss without the need for complex destructive testing by obtaining only the B-H loop using a total flux measurement system. This total flux-based main cable NDE technique can be an effective inspection tool to ensure the safety of cable-stayed structures through further research and through the convergence of robots and IT technology.

Data Availability

The raw data of the total flux signal used to support the findings of this study are available from the corresponding author upon request.

Conflicts of Interest

The authors declare that there is no conflict of interest regarding the publication of this paper.

Acknowledgments

This research was supported by the Basic Science Research Program through the National Research Foundation of Korea (NRF) funded by the Ministry of Education (NRF-2017-R1A6A3A04011933 and NRF-2017-R1A2B3007607).

References

[1] K. K. Tandon, "MFL tool hardware for pipeline inspection," *Materials Performance*, vol. 36, no. 2, pp. 75–79, 1997.

[2] C. Mandache, B. Shiari, and L. Clapham, "Defect separation considerations in magnetic flux leakage inspection," *Insight*, vol. 47, no. 5, pp. 269–273, 2005.

[3] M. L. Wang, Z. Chen, S. S. Koontz, and G. D. Lloyd, "Magnetoelastic permeability measurement for stress monitoring in steel tendons and cables," in *Proceedings Volume 3995, Nondestructive Evaluation of Highways, Utilities, and Pipelines IV*, pp. 492–500, Newport Beach, CA, USA, 2000.

[4] J. E. Lenz, "A review of magnetic sensors," *Proceedings of the IEEE*, vol. 78, no. 6, pp. 973–989, 1990.

[5] J. Lenz and S. Edelstein, "Magnetic sensors and their applications," *IEEE Sensors Journal*, vol. 6, no. 3, pp. 631–649, 2006.

[6] K. Mandal and D. L. Atherton, "A study of magnetic flux-leakage signals," *Journal of Physics D: Applied Physics*, vol. 31, no. 22, pp. 3211–3217, 1998.

[7] E. Ramsden, *Hall-Effect Sensors: Theory and Applications*, Elsevier, Newnes, Oxford, UK, 2006.

[8] S. Sumitro, A. Jarosevic, and M. L. Wang, "Elasto-magnetic sensor utilization on steel cable stress measurement," in *The First fib Congress, Concrete Structures in the 21th Century*, pp. 79–86, Osaka, Japan, 2002.

[9] M. L. Wang, G. Wang, and Y. Zhao, *Sensing Issues in Civil Structural Health Monitoring*, Springer, Dordrecht, Netherlands, 2005.

[10] H. R. Weischedel, "The inspection of wire ropes in service: a critical review," *Materials Evaluation*, vol. 43, no. 13, pp. 1592–1605, 1985.

[11] D. L. Atherton, "Magnetic inspection in key to ensuring safe pipelines," *Oil and Gas Journal*, vol. 87, no. 2, 1987.

[12] M. Goktepe, "Non-destructive crack detection by capturing local flux leakage field," *Sensors and Actuators A: Physical*, vol. 91, no. 1-2, pp. 70–72, 2001.

[13] J.-W. Kim and S. Park, "Magnetic flux leakage sensing and artificial neural network pattern recognition-based automated damage detection and quantification for wire rope non-destructive evaluation," *Sensors*, vol. 18, no. 2, pp. 109–119, 2018.

[14] H. R. Weischedel and C. R. Chaplin, "Inspection of wire ropes for offshore applications," *NDT & E International*, vol. 24, no. 6, pp. 323–367, 1991.

[15] S. Park, J.-W. Kim, C. Lee, and J. J. Lee, "Magnetic flux leakage sensing-based steel cable NDE technique," *Shock and Vibration*, vol. 2014, Article ID 929341, 8 pages, 2014.

[16] J.-W. Kim and S. Park, "Magnetic flux leakage–based local damage detection and quantification for steel wire rope non-destructive evaluation," *Journal of Intelligent Material Systems and Structures*, vol. 29, no. 17, pp. 3396–3410, 2017.

[17] S. Park, J.-W. Kim, and D.-J. Moon, "Non-contact main cable NDE technique for suspension bridge using magnetic flux-based B-H loop measurements," in *Proceedings Volume 9437, Structural Health Monitoring and Inspection of Advanced Materials, Aerospace, and Civil Infrastructure 2015*, San Diego, California, USA, 2015.

[18] C. Kittel, "Physical theory of ferromagnetic domains," *Reviews of Modern Physics*, vol. 21, no. 4, pp. 541–583, 1949.

[19] B. D. Cullity and C. D. Graham, *Introduction to Magnetic Materials*, Wiley-IEEE Press, New Jersey, USA, 2nd edition, 2011.

[20] H. A. Radi and J. O. Rasmussen, "Faraday's law, alternating current, and Maxwell's equations," in *Principles of Physics*, Springer, New York, USA, 2013.

[21] S. Chikazumi, *Physics of Ferromagnetism*, Oxford University Press, Oxford, UK, 1997.

[22] J.-W. Kim, S. Park, and D.-J. Moon, "Noncontact NDE technique for main cables of suspension bridges integrating direct current magnetization with a searching coil-based total flux measurement," *IABSE Symposium Report*, vol. 102, no. 7, pp. 2953–2960, 2014.